Available online at www.sciencedirect.com
SCIENCE DIRECT®
Coordination Chemistry Reviews 249 (2005) 859–872
COORDINATION CHEMISTRY REVIEWS
www.elsevier.com/locate/ccr

Review

The importance of the transannular secondary bonding strength in the molecular structures of metallocanes of type $[X(CH_2CH_2Y)_2MRR']$ and $[X(CH_2CH_2Y)_2M'R]$ (M = Ge(IV), Sn(IV), Pb(IV), M′ = As(III), Sb(III) and Bi(III); X = NR″, O, S; Y = O, S)

Raymundo Cea-Olivares*, Verónica García-Montalvo, Mónica M. Moya-Cabrera

Instituto de Química, Universidad Nacional Autónoma de México, Circuito Exterior, Ciudad Universitaria, México 04510 D. F., México

Available online 26 November 2004

Contents

Abstract

The 1-oxa-4,6-dithia-, 1,3,6-trithia-, 1-aza-4,6-dithia-, 1-aza-4,6-dioxa-, 1-thia-4,6-dioxa- and 1,3,6-trioxametallocanes possess a strong 1,5 transannular interaction through an acceptor atom M [Ge(IV), Sn(IV), Pb(IV), As(III), Sb(III) and Bi(III)] and an X donor (O, S, NR). The conformation adopted by the metallocane ring has exhibited various conformations along with the extreme conformations boat–boat, boat–chair and chair–chair. The structural diversity observed in these eight-membered rings results in a variety of coordination numbers, as well as in the presence of polymeric structures. The purpose of the present review is to highlight the relationship between the strength of the transannular bonding and the resulting molecular structures. Factors such as coordination number, electronegativity and steric effects are revised.

Keywords: Metallocanes; Hypervalent compounds; Transannular interaction; Eight-membered rings

1. Introduction

The eight-membered rings $X(CH_2CH_2Y)_2MRR'$ and $X(CH_2CH_2Y)_2M'R$ (M = Ge, Sn, Pb; M′ = As, Sb or Bi; X = NR″, O, S; Y = O, S) have been long studied in order to understand hypervalency of group 14 and 15 elements. Many structural determinations containing different exocyclic ligands (R and R′) have been reported, showing that these rings possess a strong 1,5 transannular interaction through the Lewis acidic acceptor M and the donor group X, leading to an increase in the coordination number of M (Scheme 1) [1].

This M···X interaction is a stabilizing factor, in contrast to the situation in the cyclooctane [2]. Some of the factors

* Corresponding author.
E-mail address: cea@servidor.unam.mx (R. Cea-Olivares).

0010-8545/$ – see front matter © 2004 Elsevier B.V. All rights reserved.
doi:10.1016/j.ccr.2004.10.002

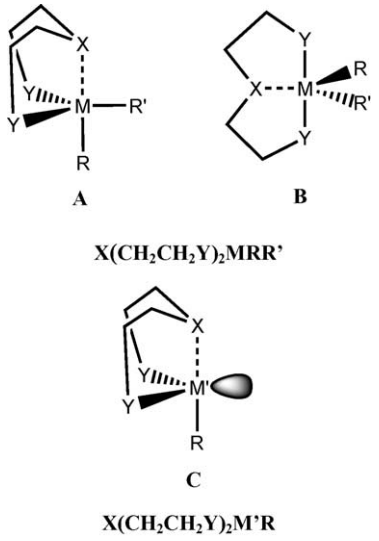

Scheme 1.

that affect the strength of the transannular bonding may be the electronegativity of the X, Y and R groups and the type of the exocyclic ligands (R/R′).

The structural diversity observed in these metallocanes results in a variety of coordination numbers and polymeric structures in the cases of heavier members of both families. The present review highlights the structural diversity observed in these types of metallocanes and revises the factors that influence the strength of transannular bonding and hypervalency at the central atom M. The survey has been divided into two sections, group 14 metallocanes [$X(CH_2CH_2Y)_2MRR'$] and group 15 metallocanes [$X(CH_2CH_2Y)_2M'R$]. The sections are organized according to the metal present in the heterocycle (M or M′, respectively). A table format was chosen to summarize the most important structural features of these complexes (e.g., bond orders, bond distances, bond angles, ring conformation, geometry, monomeric, dimeric, supramolecular associations, etc.).

2. Group 14 metallocanes

2.1. Tin(IV) metallocanes

Among the large number of structural reports of group 14 metallocanes, tin(IV) compounds are the most widely and systematically studied. Dräger et al. presented an interesting approach to understand the factors controlling the intramolecular nucleophilic attack of the donor X at the σ-Lewis acidic M (the M···X bonding). The stannocanes of type $X(CH_2CH_2S)_2SnCl_2/Br_2/I_2/Me_2$ and $X(CH_2CH_2S)_2Sn(Me)Cl/Br/I$ (X = NR, O, S) [1,3] are discussed, while the compounds $X(CH_2CH_2CH_2)_2SnR/R'$ (X= NR″; R/R′ = Cl, Br, I, $OSiPh_3$, Ph) are not considered in the scope of this review [4–6]. A model comprising a four electron-three center X···M–R_{ax} interaction was applied to explain the observations. The σ-donor X attacks at the σ*-LUMO of the acceptor M; a change of the hybridization at M occurs and, simultaneously, a transition from a tetrahedral into a trigonal-bipyramidal geometry takes place. The new LUMO is located at lower energy than the LUMO at the starting geometry. The interaction is controlled by four electronic factors: (a) the donor strength of X, (b) the electronegativity of the axial ligand, (c) the lone pair interaction of the axial ligand and (d) the nature of the equatorial ligands. In addition, steric factors related to the geometrical flexibility of X should be also considered. The results indicate that the driving force for pentacoordination results from the π-basicity of the ligands.

Structural analyses of $O(CH_2CH_2S)_2SnCl_2/Br_2/I_2/Me_2$ and $S(CH_2CH_2S)_2Sn(Me)Cl/Br/I$ (X = O, S) stannocanes reveal pentacoordinated tin atoms due to transannular coordination by the X donor atom (compounds **1**–**13**). The magnitudes of the transannular Sn···X bonds in these metallocanes and their most relevant geometrical features are listed in Table 1, together with Pauling bond orders (BO) [7]. In addition, the difference between the sum of the equatorial and axial angles [$\Delta\Sigma(\theta)$] was used to assess the position of a given structure along the trigonal-bipyramidal ↔ tetrahedral path [1,3,4,8].

In these stannocanes, the Sn···X bond lengths are larger than the sum of their covalent radii, but significantly shorter than the sum of their van der Waals radii [9]. Comparison of the BOs for Sn···X and Sn–R_{ax} indicate that the interaction between Sn and X increases with the increment of the electronegativity of the axial ligand. Nonetheless, this tendency is not followed in the case of compounds $S(CH_2CH_2S)_2Sn(Me)Cl/Br$ (**10** and **12**). The BO (Sn···X) is slightly larger for the stannocane containing Br as the axial ligand compared to the chloride, though these differences may be at the borderline of statistical significance. This inversion of the *trans* influence reveals the importance of the π-basicity of the ligand controlling the path. All the compounds containing halogens as exocyclic ligands are in the same range of hypervalency. Furthermore, if a halogen atom at an equatorial position is replaced by a methyl group, a decrease in the BO (Sn···X) occurs. A similar phenomenon is observed when the axial halogen ligand is exchanged by a methyl group, as in the case of $X(CH_2CH_2S)_2SnMe_2$ (**7** and **8**). In addition, compound **8** exhibits a heptacoordinate tin atom due to the anticipated Sn···S transannular bonding and to two additional intermolecular contacts with the sulfur atoms from the neighboring molecules [Sn···S1′ = 3.678(2) Å and Sn···S3′ = 4.097(2) Å]. The resulting polyhedron can be described as a tricapped tetrahedron with the secondary bonds at the capping sites.

A regular trend is the presence of a chair–chair (CC) conformation in all the 1-oxa-4,6-dithia-stannocanes, while, the 1,3,6-trithia-stannocanes display a boat–chair (BC) conformation (Scheme 2). Moreover, in the chair–chair conformation, the endocyclic angle is the largest of the equatorial angles present at the tin atom. The endo–exo equatorial angle is the largest at the tin atom for a boat–chair conformation,

Table 1
Structural features of the three center interaction X··· M–R_{ax} for the group 14 compounds, $X(CH_2CH_2Y)_2MRR'$ (M = Ge, Sn, Pb)

Compound	d(M···X) Å	Δd[a]	BO[b] M···X	d(M–R_{ax}) Å	BO[a,b] M–R_{ax}	X···M–R_{ax} (Deg.)	Δ Σ(θ)[c] (Deg.)	Conformation	References
$O(CH_2CH_2S)_2SnCl_2$, **1**	2.359(6)	0.299	0.37	2.376(3)	0.95	170.9(2)	60.5	CC	[1]
$S(CH_2CH_2S)_2SnCl_2$, **2**	2.760(3)	0.32	0.35	2.392(3)	0.99	165.6(1)	70.1	BC	[1]
$O(CH_2CH_2S)_2SnBr_2$, **3**	2.41(1)	0.35	0.32	2.536(2)	0.92	165.8	59.0	CC	[1]
$S(CH_2CH_2S)_2SnBr_2$, **4**	2.767(2)	0.32	0.34	2.545(1)	0.9	174.5(1)	69.9	BC	[1]
$O(CH_2CH_2S)_2SnI_2$, **5**	2.431(5)	0.37	0.3	2.738(1)	0.83	166.4(1)	51.0	CC	[1]
$S(CH_2CH_2S)_2SnI_2$, **6**	2.779(2)	0.34	0.33	2.786(1)	0.71	177.6(1)	70.1	BC	[1]
$O(CH_2CH_2S)_2SnMe_2$, **7**	2.774(5)	0.714	0.09	2.183(8)	0.9	163.6(3)	37.4	CC	[3]
$S(CH_2CH_2S)_2SnMe_2$, **8**	3.514(1)	1.07	0.03	2.147(3)	1	169.3(1)	55.4*	BC	[3]
$O(CH_2CH_2S)_2SnClMe$, **9**	2.42(2)	0.36	0.31	2.413(1)	0.92	168.3(5)	59.8	CC / BC	[3]
$S(CH_2CH_2S)_2SnClMe$, **10**	2.863(1)	0.423	0.25	2.444(1)	0.84	168.6(3)	72.0	BC	[3]
$O(CH_2CH_2S)_2SnBrMe$, **11**	2.440(4)	0.38	0.29	2.561(1)	0.84	166.5(1)	56.4	CC	[3]
$S(CH_2CH_2S)_2SnBrMe$, **12**	2.835(2)	0.4	0.28	2.582(1)	0.8	168.52(4)	73.3	BC	[3]
$O(CH_2CH_2S)_2SnIMe$, **13**	2.466(3)	0.4	0.26	2.762(1)	0.77	167.0(1)	52.8	CC	[3]
$O(CH_2CH_2S)_2SnPhMe$, **14**	2.677(5)	0.617	0.13	2.150(3)	1	167.9(4)	34.4	CC	[10]
$O(CH_2CH_2S)_2SnPh_2$, **15**	2.66(7)	0.6	0.14	2.147(7)	1	168.8(3)	35.7	Monoplanar	[11]
$S(CH_2CH_2S)_2SnPh_2$, **16**	3.246(1)	0.8	0.07	2.156(3)	0.98	170.8(1)	31.0	BC	[12]
$O(CH_2CH_2S)_2SnClPh$, **17**	2.41(1)	0.35	0.30	2.453(1)	0.81	167.3(4)	62.7	Diplanar	[13]
$S(CH_2CH_2S)_2SnClPh$, **18**	2.866(2)	0.36	0.30	2.453(1)	0.81	174.2(1)	73.3	BC	[14]
$O(CH_2CH_2S)_2SnCl(nBu)$, **19**	2.409(7)	0.349	0.32	2.407(3)	0.95	169.7(2)	62.0	BC	[32]
$S(CH_2CH_2S)_2SnCl(nBu)$, **20**	2.785(1)	0.345	0.32	2.446(5)	0.83	170.22(6)	80.9	BC	[32]
$O(CH_2CH_2S)_2SnCl$-$(S_2CNC_4H_6)$, **21**	2.727(11)	0.89	0.05	2.493(1)	0.84	139.01(9)[d]		CC	[15]
						153.8(1)	86.2		
$O(CH_2CH_2S)_2Sn(nBu)$-$(S_2CNC_4H_6)$, **22**	2.723(4)	0.66	0.11	2.490(6)	0.85	158.92(11)	42.1	BC	[15]
$S(CH_2CH_2S)_2Sn(nBu)$-$(S_2CNC_4H_6)$, **23**	3.175(1)	0.734	0.09	2.517(2)	0.79	164.44(4)		BC	[15]
$O(CH_2CH_2S)_2Sn$-$(S_2CNC_4H_6)_2$, **24**	3.229(5)	1.17	0.022	2.612(2)	0.6	141.55(9)[d]		BC	[15]
						(158.54(7))	44.1		
$O(CH_2CH_2S)_2Sn(nBu)$-$(S_2CNC_4H_8)$, **25**	2.763	0.703	0.1	2.498(3)	0.83	156.9(7)	41.7	BC	[16]
$O(CH_2CH_2S)_2Sn(nBu)]_2R$, **26**; R =$(S_2CNC_4H_8NCS_2)$	2.688(3))	0.628	0.13	2.509(3)	0.8	159.9(2)	34.3	BC	[17]
$O(CH_2CH_2S)_2Sn(nBu)$-$(S_2PO_2C_3H_4Et_2)$, **27**	2.468(8)	0.41	0.26	2.509(3)	0.8	163.0(2)	58.1	BC	[18]
$S(CH_2CH_2S)_2Sn(nBu)$-$(S_2PO_2C_3H_4Et_2)$, **28**	2.940(7)	0.505	0.2	2.538(3)	0.72	166.0(2)	63.7	BC	[18]
$O(CH_2CH_2S)_2Sn(nBu)R$, **29**; R =-$(S_2PO_2CHMeCH_2CHMe)$	2.555(2)	0.495	0.2	2.496(4)	0.83	162.34(5)	52.51	BC	[17]
$S(CH_2CH_2S)_2Sn(nBu)R$, **30**; R =-$(S_2PO_2CHMeCH_2CHMe)$	2.982(2)	0.542	0.17	2.527(2)	0.75	166.75(6)	63.65	BC	[17]
$S(CH_2CH_2S)_2Sn$-$(S_2P(OiPr)_2(nBu)$, **31**	3.027(1)	0.582	0.15	2.526(1)	0.75	164.5(5)	54.4	BC	[15]
$[O(CH_2CH_2S)_2Sn$-$(S_2CNMe_2)R$, **32**; R = $(C_2H_4C(O)OMe)$	2.625(2)	0.55	0.16	2.492(1)	0.84	159.9(1)	49.3	BC	[19]
$[O(CH_2CH_2S)_2]_2Sn$, **33**	2.776(4)	0.716	0.098	2.412(2)	1.09	165.36(14)	23.6	BC	[20]
(molecules a and b)	2.837(4)	0.777	0.08	2.412(2)	1.09	163.62(13)			
	2.758(4)	0.698	0.103	2.416(2)	1.08	166.51(12)			
	2.900(4)	0.84	0.065	2.403(4)	1.1	164.14(12)	28.5		
	2.837(4)	0.777	0.08	2.412(2)	1.09	163.62(13)			

Table 1 *(Continued)*

Compound	d(M···X) Å	Δd[a]	BO[b] M···X	d(M–R_{ax}) Å	BO[a,b] M–R_{ax}	X···M–R_{ax} (Deg.)	Δ$\Sigma(\theta)$[c] (Deg.)	Conformation	References
$[S(CH_2CH_2S)_2]_2Sn$, **34**	3.074(3)	0.637	0.13	2.434(2)	1.021	170.73(10)	36.4	BC	[20]
	3.241(3)	0.8	0.07	2.424(2)	1.05	167.78(11)			
$O(CH_2CH_2S)_2Sn(SCH_2)_2$, **35**	2.529(5)	0.469	0.22	2.412(3)	1.09	172.5(2)	46.9	BC	[21]
(molecules a and b)	2.454(6)	0.394	0.28	2.418(3)	1.08	174.5(3)	52.0		
$S(CH_2CH_2S)_2Sn(SCH_2)_2$, **36** (molecules a and b)	2.815(1)	0.375	0.29	2.444(2)	0.99	174.16(8)	62.23	BB	[22]
	2.840(1)	0.4	0.27	2.426(2)	1.05	173.97(9)	65.4	BC	
$MeN(CH_2CH_2O)_2Sn(tBu)_2$, **37** (molecules a,b,c)	2.33(1)	0.23	0.47	2.05(1)	1.03	150.1(5) d	87.5	double	[8]
	2.30(1)	0.2	0.52	2.05(1)	1.03	150.2(5)	84.8	envelope	
	2.34(2)	0.24	0.46	2.02(1)	1.03	151.3(6)	91.8		
$MeN(CH_2CH_2S)_2SnMe_2$, **38**	2.566(6)	0.466	0.22	2.16(1)	0.97	165.8	55.4	BC	[3,23]
$MeN(CH_2CH_2O)_2Sn(S_2CNMe)R$, **39**; R = $(C_2H_4C(O)OEt$	2.322(7)	0.22	0.48	2.09(1)	1.2	173.5(4)	64.7	BC	[19]
$[MeN(CH_2CH_2S)_2SnPh]_2CH_2$, **40** (rings a and b)	2.651(7)	0.551	0.167	2.179(8)	0.91	166.4(3)	56.4	Monoplanar BC	[38]
	2.654(7)	0.554	0.165	2.162(7)	0.96	162.8(3)	48.77		
$[HOCH2CH2N(CH_2CH_2O)_2]_2Sn$, **41** β	2.332(10)	0.232	0.47	2.034(10)	1.08	165.0(3)	66.5	BC	[33]
(α- and crystal forms)	2.383(10)	0.283	0.398	2.041(10)	1.06	164.6(3)	67.5	BC	
α	2.33(1)	0.23	0.473	2.01(1)	1.1	169.5(2)	71.1	BB	[34]
$O(CH_2CH_2S)_2GeCl_2$, **42**	2.36(1)	0.48	0.21	2.212(4)	0.99	172.8(3)	60.8	CC	[25]
(molecules a and b)	2.39(1)	0.51	0.2	2.204(4)	1.02	169.3(3)	62.7		
$S(CH_2CH_2S)_2GeCl_2$, **43**	3.01	0.75	0.08	2.208(3)	1	182.2	54.2	BC	[26]
$O(CH_2CH_2S)_2GeSO(C_2H_4)$, **44**	2.492(3)	0.612	0.14	1.806(2)	1.27	176.2(1)	56.26	BC	[21]
$S(CH_2CH_2S)_2GeSO(C_2H_4)$, **45**	2.842(1)	0.582	0.15	1.796(3)	1.3	174.96(7)	64.02	BC	[21]
$O(CH_2CH_2S)_2Ge(SCH_2)_2$, **46**	2.616(1)	0.736	0.09	2.226(8)	1.11	173.41(4)	42.01	BC	[21]
$[O(CH_2CH_2S)_2]_2Ge$, **47**	2.914(3)	1.034	0.036	2.218(1)	1.1	169.0(5)	21.4	BC	[27]
(molecules a and b)	3.040(3)	1.16	0.023	2.17(1)	1.3	166.7(5)			
	2.955(3)	1.07	0.03	2.217(1)	1.3	168.7(5)	22.3		
	2.946(3)	1.06	0.03	2.222(1)	1.1	168.4(4)			
$[S(CH_2CH_2S)_2]_2Ge$, **48**	3.237(3)	0.977	0.042	2.236(3)	1.1	174.5	27.4	BC	[27]
	3.453(3)	1.193	0.02	2.210(3)	1.1	170.8			
$MeN(CH_2CH_2O)_2Ge(OCH_2)_2$, **49**	2.159(3)	0.24	0.46	1.808(3)	1.2	178.6(4)	75.2	BC	[28]
$MeN(CH_2CH_2O)_2GeO_2(C(OH)C(Ph_2))$, **50**	2.080(4)	0.16	0.6	1.870(4)	1.03	178.0(3)	85.2	BC	[29]
$MeN(CH_2CH_2O)_2Ge(OH)_2$, **51**	2.123(4)	0.21	0.5	1.793(3)	1.3	177.9(2)	70.6	BC	[30]
$O(CH_2CH_2S)_2PbPh_2$, **52**	2.855(5)	0.745	0.09	2.197	0.86	157.8(2)	23.0	CC	[31]
Orthorhombic crystal (molecules a and b)	2.888(6)	0.778	0.08	2.194	0.86	161.1(3)	20.8	CC	
Triclinic crystal (molecules a and b)	2.92(1)	0.81	0.07	2.21	0.82	158.7(3)	16.0	CC	
	3.08((1)	0.97	0.04	2.2	0.85	163.2(3)	12.2	BC	

[a] Bond widening, $\Delta d = (d_{exp} - \Sigma r_{Cov})$, according to standard bond distances d(Ge—N) 1.92, d(Ge—O) 1.88, d(Ge—S) 2.26, d(Ge—Cl) 2.21, d(Sn—N) 2.10, d(Sn—O) 2.06, d(Sn—S) 2.44, d(Sn—Cl) 2.39, d(Sn—Br) 2.51, d(Sn—I) 2.68, d(Sn—C) 2.15 [9], d(Pb—O) 2.11, d(Pb—S) 2.51 Å [31].

[b] Mode of calculation $BO = 10^{-(1.41\Delta d)}$ [3,7].

[c] $\Delta\Sigma(\theta) = \Sigma\theta_{eq} - \Sigma\theta_{ax}$, difference between the angles becoming equatorial and axial during the transition of a perfect tetrahedron ($\Delta\Sigma(\theta) = 0°$) to a perfect trigonal bipyramid ($\Delta\Sigma(\theta) = 90°$) [1,3,4,8].

[d] The largest angle does not correspond to X···M–R_{ax} but to Cl—Sn—S1(L) (**21**) and S—Sn···S2(L) (**24**) O1—Sn—O2 (**37**) [15].

demonstrating the influence of the steric factors related to the nature of the X donor [1,3]. On the other hand, stannocane $O(CH_2CH_2S)_2SnClMe$ (**9**) exhibits a splitting of the atoms C1 and C2 in the eight-membered ring. The analysis of the disordered atoms revealed the presence of both the chair–chair and boat–chair conformation in the same crystal structure.

The series $X(CH_2CH_2S)_2Sn(Ph)Ph/Me$ and $X(CH_2CH_2S)_2Sn(Cl)Ph/nBu$ (X = O, S) show similar trends (compounds **14–20**, Table 1) [10–14,33]. The strength of the Sn···X interaction decreases when the halogen atoms are partially or totally replaced by methyl, *n*-butyl or phenyl groups. Exchange of both exocyclic ligands in $X(CH_2CH_2S)_2SnMe_2$ [X = O (7), X = S (**8**)] leads to a notable decrease in the BO (Sn···X) compared to the BOs found in the dihalogen and in the partially substituted derivatives. The lowest BO (Sn···X) and the highest BO ($Sn–R_{ax}$) are those corresponding to compounds that do not contain halogens as exocyclic ligands (**7**, **8**, **14–16**). In the case of compound $O(CH_2CH_2S)_2SnPhMe$ (**14**), the phenyl group occupies the axial position. Moreover, according to the geometrical parameters collected in Table 1, the coordination geometries of these four stannocanes (**7**, **8**, **14–16**) are markedly deviated from the ideal trigonal-bipyramid.

The chlorine containing stannocanes $X(CH_2CH_2S)_2Sn(Cl)Ph/nBu$ [X = O (**17** and **19**), X = S (**18** and **20**)] have BO (Sn···X) and BO ($Sn–R_{ax}$) in the same range as those of the halogen-containing stannocanes discussed initially. Derivatives $X(CH_2CH_2S)_2SnCl(nBu)$ [X = O(**19**), S(**20**)] exhibit shorter Sn···X bond lengths (BO 0.32) than those of methyl and phenyl $X(CH_2CH_2S)_2SnClMe/Ph$ homologues. This comparison is more evident in the case of the 1,3,6-trithia-stannocanes **10** and **18** (Table 1).

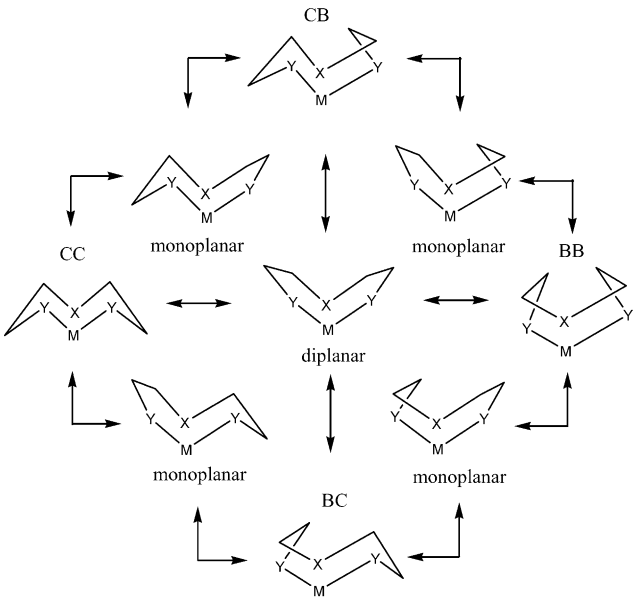

Scheme 2.

On the other hand, the 1-oxa-4,6-dithia-stannocanes $O(CH_2CH_2S)_2SnPh/Ph/Cl$ (**15** and **17**) exhibit peculiar ring conformations. Compound $O(CH_2CH_2S)_2SnPh_2$ (**15**) shows a monoplanar ring arrangement, which corresponds to the path between a chair–chair and a boat–chair conformation (Scheme 2). The diplanar arrangement found in $O(CH_2CH_2S)_2SnClPh$ (**17**) is indicative of a transition between the two enantiomers of the boat–chair conformation. It is opportune to mention that the $O(CH_2CH_2S)_2SnCl(nBu)$ (**19**) is the first example in these 1-oxa-4,6-stannocanes that exhibits a boat–chair ring conformation, all the previous oxa-analogous compounds have shown a chair–chair ring arrangement. As in the case of the previous examples, it is clear from the geometrical parameters listed in Table 1 that the tin coordination geometry deviates much more from the ideal trigonal-bipyramid in the case of 1-oxa-4,6-dithia-stannocanes, where the X donor atom corresponds to oxygen.

Compounds **21–32** listed in Table 1 are nonsymmetrically substituted stannocanes of type $X(CH_2CH_2S)_2Sn(Cl/R/L)L$ (X = O, S; R = nBu, $CH_2CH_2C(O)OMe$) [15–19]. The L represents a bidentated monoanionic ligand such as the dithiolates $[S_2P(OR)_2]^-$, $[S_2CNR_2]^-$, and the bridging ligand $[S_2CN(CH_2CH_2)_2NCS_2]^{2-}$. Several remarkable features are interesting to note in these compounds. All the eight-membered rings with exception of $O(CH_2CH_2S)_2SnCl(S_2CNC_4H_6)$ (**21**), exhibit a boat–chair conformation. The eight-membered ring in **21** displays a chair–chair conformation, which is a common feature in the 1-oxa-4,6-dithia-stannocanes analyzed, but other stannocanes containing oxygen as the X donor atom display different types of conformations. Dithiolate ligands coordinate to the tin atom asymmetrically (anisobidentate mode) leading to one primary Sn–S1(L) bond and to a secondary Sn···S2(L) bond. This exocyclic Sn···S2(L) intramolecular interaction is usually weaker than the transannular Sn···X bond. In general, the primary Sn–S1(L) bond and the transannular Sn···X interaction correspond to the axial bonds, with the exception of $O(CH_2CH_2S)_2SnCl(S_2CNC_4H_6)$ (**21**) and $O(CH_2CH_2S)_2Sn(S_2CNC_4H_6)_2$ (**24**), in which the largest angles correspond to the Cl–Sn–S1(L) and S–Sn···S2(L) angles [153.8(1)° and 158.54(7)°, respectively] [15]. Consequently, in these compounds the transannular Sn···X bonds occupy equatorial positions. The last important feature in these compounds corresponds to the hexacoordinated tin environment, where four primary bonds form a distorted bicapped tetrahedron. The X atom of the transannular Sn···X bond and the sulfur atom belonging to the secondary Sn···S(L) bond cap the tetrahedron. $O(CH_2CH_2S)_2Sn(S_2CNC_4H_6)_2$ (**24**) represents the only exception, in which the tin atom is heptacoordinated with a transannular Sn···O bond and the two secondary Sn···S2(L) bonds capping three faces of a Ψ-tetrahedron. It seems that the presence of exocyclic bidentate ligands leads to a decrease in the transannular M···X bond, along with a higher distortion of the geometrical arrangement of the metal center (Table 1).

Spiro-stannocanes **33**–**36** are listed in Table 1 [20–22]. The BO (Sn···X) found in the symmetric spiro-stannocanes **33** and **34** are in the same range as those encountered in stannocanes containing methyl and/or phenyl groups as exocyclic ligands. In these two compounds one of the Sn···X bond distances is slightly shorter than the other. In addition, the geometry around both tin atoms is closer to a tetrahedron, with the X donor atoms capping two of the faces of the distorted polyhedron.

On the other hand, in the asymmetric spiro-stannocanes **35** and **36** [21,22], the BOs (Sn···X) are in the range of those found for the L-containing stannocanes, where the Sn–S1(L) bond and the Sn···X interaction correspond to the axial positions. The eight-membered rings exhibit a boat–chair arrangement in almost all theses cases, only one of the independent molecules for $S(CH_2CH_2S)_2Sn(SCH_2)_2$ (**36**) exhibits a boat–boat conformation. The later is hitherto, the only example of a boat–boat conformation in any known stannocane (Fig. 1).

Finally, it is important to mention the main structural features of aza-stannocanes (37–41), which have two principal features of interest. First, the strength of the transannular Sn···N interaction increases markedly in comparison with the transannular Sn···S and Sn···O bonds. By comparing the BOs (Sn···N) for **37** (0.46–0.52), **38** (0.22), **39** (0.48) and **41** (0.40–0.47), it is clear that the reduction observed in $MeN(CH_2CH_2S)_2SnMe_2$ (**38**) is associated with the presence of S atoms, which possess lower electronegativity than the oxygen atoms within the eight-membered rings of **37**, **39** and **41**. The BO (Sn···N) in **37** is the highest known value for any reported stannocane. The second interesting feature deals with the occurrence of the two basic trigonal-bipyramidal configurations in the solid state (A) and (B) (Scheme 1) [8,24]. It seems that this feature depends on the nature of the groups involved in the molecular makeup. $MeN(CH_2CH_2O)_2Sn(tBu)_2$ (**37**) exhibits a B type configuration [8], representing the first example of an equatorial Sn···N dative bond for a pentacoordinated tin compound. The main distortion from the ideal trigonal-bipyramid in **37** is the small apical O–Sn–O angle (average 150.5°). Moreover, the eight-membered ring in this compound displays a very peculiar arrangement referred to as a "double envelope", due to the two fused five-membered rings. In contrast, the two aza-stannocanes $MeN(CH_2CH_2S)_2SnMe_2$ (**38**) and $MeN(CH_2CH_2O)_2Sn(S_2CNMe)(C_2H_4C(O)OEt$ (**39**) exhibit the conventional A configuration (Scheme 1) and a boat–chair conformation [3,19,23]. The strength of the Sn···N bond in the analogous Sn(II) compound tBu-$N(CH_2CH_2S)_2SnCr(CO_5)$ [40] differs only slightly in comparison with **38**, while in the case of $[tBu\text{-}N(CH_2CH_2S)_2Sn]_2$ [41], the Sn···N bond is considerably weaker (BO 0.06–0.17). This may be explained by the involvement of the tin atom in the formation of dimeric structures through Sn_2S_2 rings.

On the other hand, the aza-stannocane $[HO(CH_2)_2N(CH_2CH_2S)_2]Sn$ (**41**) crystallized dimorphically as α- and β-modifications [33,34]. Some important features are interesting to note. First, the triethanolamine behaves as a tridentated ligand in **41**, while it acts as a tetradentate ligand in silicon and zinc complexes [35–37]. Second, the BO (Sn···N) is within the same range of values as other aza-stannocanes, contrasting the striking decrease in the BO (Sn···X) of oxa- and trithia-spirostannocanes (**33** and **34**). Moreover, the tin coordination geometry in **41** is best described as an octahedron rather than a bicapped tetrahedron as in the cases of **33** and **34**. It is also important to note that the eight-membered rings in the α-crystalline form exhibit a boat–boat conformation (Fig. 2).

In contrast to the bridged system in **26**, where the two eight-membered rings are equivalent, in the aza-derivative $[MeN(CH_2CH_2S)_2SnPh]_2CH_2$ (**40**) [38] the phenyl group occupies an axial position in one of the rings (*a*) and an equatorial site in the other ring (*b*), while the methylene bridge is either in an equatorial or in an axial position. Another im-

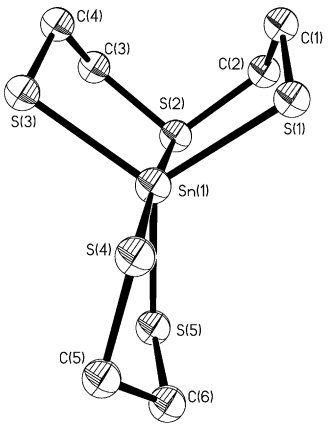

36a

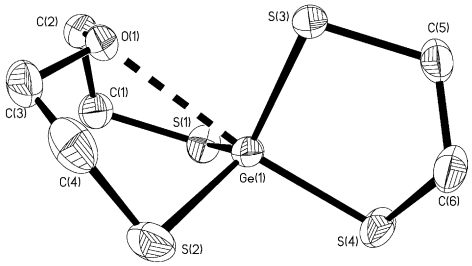

44

Fig. 1. Molecular structures of $S(CH_2CH_2S)_2Sn(SCH_2)_2$ (**36**, molecule a, BB) and $O(CH_2CH_2S)_2Ge(SCH_2)_2$ (**46**, BC).

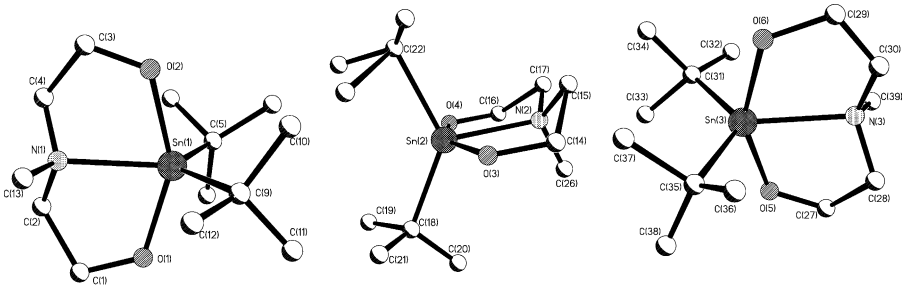

37a **37b** **37c**

Fig. 2. Molecular structures of $MeN(CH_2CH_2O)_2Sn(tBu)_2$ (**37**, molecules a, b and c).

portant feature to note, is the conformation adopted by the two eight-membered ring moieties. Ring a can be described as in transition between the boat–chair and chair–chair conformation (see Scheme 2), while ring *b* adopts a boat–chair arrangement. Both nitrogen atoms in **40** are in the axial positions and the Sn···N bond lengths are slightly larger than that found in the analogous $MeN(CH_2CH_2S)_2SnMe_2$ (**38**), but are comparable to the Sn···O bond distances observed in stannocanes containing phenyl groups as exocyclic ligands (**14** and **15**).

Comparison of structural data among organometallic stannocanes of type $X(CH_2CH_2CH_2)_2SnRR'$ (X = NR″, O, S; R/R′ = Cl, Br, I, $OSiPh_3$, Ph) and their $X(CH_2CH_2Y)_2SnRR'$ homologues [4–6] brings forth important issues. In contrast to the trend observed in $X(CH_2CH_2Y)_2SnRR'$ stannocanes, the Sn···X interaction increases with decreasing electronegativity of the axial ligands. For $X(CH_2CH_2CH_2)_2SnCl_2$ compounds, the BO (Sn···X) and BO ($Sn–Cl_{ax}$) follow the order NMe > NBu^i > NBz> O> S and S> NMe> O> NBu^i > NBz, respectively. Therefore, an inversion of the *trans* influence holds for the donor sequence NBz–NBu^i –NMe, and also for compounds $O(CH_2CH_2CH_2)_2SnCl_2$ and $O(CH_2CH_2CH_2)_2SnBr_2$. In the case of $X(CH_2CH_2CH_2)_2SnCl_2$ (X = O, S), a normal *trans* influence is observed, as well as for compounds $R''N(CH_2CH_2CH_2)_2SnCl_2$, $R''N(CH_2CH_2CH_2)_2Sn(OSiPh3)_2$, $R''N(CH_2CH_2CH_2)_2SnCl_2$ and $R''N(CH_2CH_2CH_2)_2SnClPh$. These results illustrate the importance of the counteractive effects of a σ-donor attack and the π-basicity of the axial ligand in the control the nucleophilic attack path.

2.2. Germanium(IV) metallocanes

Germanium metallocanes (germocanes) exhibit most of the same trends that are observed in stannocanes, although available structural data are scarce. 1-oxa-4,6-dithia-germocanes (i.e., **42**) exhibit chair–chair arrangements, while 1,3,6-trithia-germocanes (i.e., **43**) display boat–chair conformations, both cases are similar to those observed in the stannocane homologues. A remarkable decrease occurs in the BO of the transannular Ge···X, when the donor atoms are exchanged from O to S in compounds $X(CH_2CH_2S)_2GeCl_2$, [X = O (**42**), S (**43**)] (Table 1) [25,26]. However, this trend is reverted in other germocanes, as can be seen in the examples listed in Table 1.

In the case of the asymmetric spiro-germocanes $O(CH_2CH_2S)_2GeSO(C_2H_4)$ (**44**), $S(CH_2CH_2S)_2GeSO(C_2H_4)$ (**45**) and $O(CH_2CH_2S)_2Ge(SCH_2)_2$ (**46**) (Table 1), the transannular Ge···X bond is stronger for the 1-oxa-4,6-dithia-germocanes (**44** and **46**) than for the 1,3,6-trithia derivative (**45**), this same trend is observed in the stannocane homologues [21]. Comparison between the homologue spiro-compounds $O(CH_2CH_2S)_2Ge(SCH_2)_2$ (**46**, Fig. 1) and $O(CH_2CH_2S)_2Sn(SCH_2)_2$ (**35**) brings forth the fact that the BO (M···O) is higher for the tin metallocane. This can be accounted for by the decrease of the LUMO with higher atomic number of the central atom similar to that observed in the homologue $R''N(CH_2CH_2CH_2)_2MRR'$ compounds [5,39]. In addition, exchange of the axial ligand in 1-oxa-4,6-dithia-germocanes shows that the BO (Ge···X) is higher when the axial atom is oxygen instead of sulfur, as can be seen in compounds **44** (BO, 0.14) and **46** (BO, 0.09). On the other hand, as for halogen-containing stannocanes, an inversion or ceasing of the *trans* influence is observed for these examples. In the asymmetric spiro-germocanes, the germanium atom displays a pentacoordinate environment, similar to that exhibited in the homologue spiro-stannocanes. The symmetric spiro-germocanes $[X(CH_2CH_2S)_2Ge]_2$ (**47** and **48**) [27] display very weak BOs (Ge···X), in comparison with those of related structures, as encountered for spiro-stannocane **30**. The symmetric spiro-germocanes exhibit hexacoordinate germanium mainly due to the presence of two transannular Ge···X bonds. The arrangement in these compounds is best described as a bicapped tetrahedron, with each eight-membered ring showing a boat–chair conformation.

In the case of the aza-germocanes $MeN(CH_2CH_2O)_2Ge(OCH_2)_2$ (**49**), $MeN(CH_2CH_2O)_2GeO_2[C(OH)C(Ph_2)]$ (**50**) and $MeN(CH_2CH_2O)_2Ge(OH)_2$ (**51**) [20,28,29], the BOs (Ge···N) are remarkably high as for their tin homologues. This striking increase in the strength of the Ge···N

bond is not only due to the presence of N as the donor atom, but also to the presence of the more electronegative oxygen atoms in both the equatorial and axial positions. The pentacoordinate geometry at germanium deviates the least from the ideal trigonal-bipyramid for these three compounds, with regard to the other germocanes (Table 1). The eight-membered rings exhibit boat–chair conformations in these compounds.

2.3. Lead(IV) metallocanes

The only reported structure of a plumbocane corresponds to the oxa-derivative $O(CH_2CH_2S)_2PbPh_2$ (**52**) [31]. Compound **52** crystallizes dimorphically as orthorhombic and triclinic crystals. Both types of crystal present two crystallographic independent molecules. This compound exhibits low BOs (P···O) indicating weak transannular P···O bonding, however, the Pb···O bond lengths are still significantly shorter than the sum of their van der Waals radii. The triclinic crystal exhibits slightly larger Pb···O bond lengths, probably due to the involvement of the lead atom in additional intermolecular Pb···S contacts. These Pb···S contacts are larger (average 3.93 Å) than the transannular Pb···O bonds and lead to the formation of dimeric units. The coordination geometry around the Pb atom can be best described as a bicapped tetrahedron. The two independent molecules exhibit different ring conformations; chair–chair and boat–chair. In contrast, the orthorhombic crystals display monocapped tetrahedral geometries at the lead atoms, with no evidence of intermolecular contacts. In this case, both eight-membered rings display the same type of chair–chair conformation. According to the $\Delta\Sigma(\theta)$ criterion, this plumbocane is the metallocane of this family that deviates the most from the ideal trigonal-bipyramid geometry (Table 1).

3. Group 15 metallocanes

A relatively large number of group 15 metallocanes $[X(CH_2CH_2Y)_2MR$, M = Ar, Sb; Y = O, S] have been prepared and structurally investigated both in solution and in the solid state. With one exception (compound **86**, which corresponds to a 1,3,5-triaza-bismocane) the scope of this review is limited to 1-oxa-4,6-dithia- and 1,3,5-trithia-metallocanes containing As, Sb and Bi.

3.1. Arsenic(III) metallocanes

Comparison of the structural data for halogen-containing arsocanes reveals different trends in the strength of the X donor σ-Lewis acidic metal interaction, [where X = O and S; and the metal center corresponds to AsR_{ax}, (R = halogen)]. The M···X distances and calculated BOs (Table 2) indicate that the strength of the transannular $X\cdots AsR_{ax}$ interaction follows 1-oxa-4,6-dithia-arsocanes; O···AsCl (**53**) > O···AsI (**55**) > O···AsBr (**54**), whereas for 1,3,6-trithia-arsocanes S···AsBr (**62**) > S···AsCl (**60**) > S···AsI (**63**). In general, halogen-containing arsocanes exhibit relatively strong transannular bonding (BO 0.21 for **62**) to very weak bonding (BO 0.09 for **54**). This order is not governed by the electronegativity of the R ligand (influence of the HOMO). Instead, an enhanced $n\sigma^*$ or $\pi\sigma^*$ charge transfer from R_{ax} into the LUMO of the π-acidic M promotes the path. The sequence in the M···X interaction of these arsocanes suggests that the electronegativity of the ligand and the $n\sigma^*$ charge transfer into the LUMO of the metal center are counteractive. A similar phenomenon is observed in the group 14 homologues, but substantial differences are encountered in features such as, geometry and solid frameworks.

Geometrically, a continuous change from a ψ-tetrahedral tricoordination to a ψ-trigonal bipyramidal tetracoordination occurs in these compounds. Nonetheless, the measurement of a trigonal-bipyramidal ↔ tetrahedral path ($\Delta\theta$) does not represent an optimal instrument for the estimation of the degree of distortion from an idealized geometry. Furthermore, when used for the description of the geometry of the heavier elements, antimony and bismuth, $\Delta\theta$ does not fit within the range of the calculated values. This is due mainly to the existence of intermolecular bonding in the heavier elements. Other methods used to estimate the degree of distortion from an idealized geometry include measurement of dihedral angles [42]. Yet, there is no ideal model to date to assess this phenomenon.

The molecular structures of arsocanes that contain dithiolate ligands exhibit anisobidentate coordination modes that lead to a decrease in the transannular BO (As···X), along with a higher distortion in the geometry of the metal center. The most important structural features of these compounds are summarized in Tables 2 and 3. The coordination geometry at arsenic in these types of compounds is difficult to describe. If secondary interactions are neglected, the arsenic atom displays the usual trigonal-pyramidal geometry, but with nonequivalent bond angles. Nevertheless, the steric influence of the secondary bonds cannot be ignored. In all of these compounds, the severe distortions from the idealized geometries can be ascribed to; constraints within the eight-membered ring, lone pair bonding repulsion and to the small S–As···S angle value (formed by anisobidentate chelation of arsenic with the dithiolate ligand). Therefore, perfect geometric arrangements like C (Scheme 1) are seldom observed in this family, especially in the cases of the heavier members.

In this regard, comparison of the sum of the dihedral angle values $[\Sigma_i|\delta_i(M) - \delta_i\ (TBP)|]$, with the sum $[R = \Sigma_i|\delta_i(TBP) - \delta_i\ (SPY)|]$ [42] for the two idealized geometries allows the assessment of the percentage of displacement between the two geometries—trigonal bipyramidal (TBP) and square pyramidal (SPY). A dihedral angle plot obtained from the application of this method on a common reference scale (if the Berry coordinate is followed) must go from 0 to 217°. For the majority of the dithiolate-containing arsocanes, the calculated dihedral angles range from 206 to

Table 2
Structural features of the three center interaction X···M′–R_{ax} for the arsenic andantimony rings, $X(CH_2CH_2Y)_2M'R$ (M = As, Sb)

Compound	d(M···X)[a] Å	BO[b] M···X	d(M···S)[a] Å	BO[c] M···S	d(M–R_{ax})[a] Å	BO[b] M–R_{ax}	$\Delta\theta$ (deg[c].)	X···M–R_{ax} (deg.)	Conformation	References
$O(CH_2CH_2S)_2AsCl$, **53**	2.451(6)	0.156	–	–	2.269	0.725	12.5	191.6	BC	[47]
$O(CH_2CH_2S)_2AsBr$, **54**	2.59	0.099	–	–	2.40	0.699		–	–	[46]
$O(CH_2CH_2S)_2AsI$, **55**	2.46	0.152	–	–	2.65	0.540		–	–	[46]
$O(CH_2CH_2S)_2AsS_2CN$-$(CH_2CH_2)_2O$, **56**	2.957(4)	0.027	3.026(2)	0.073	2.280(2)	0.429	11.2	154.3(.1)	BC	[43]
$O(CH_2CH_2S)_2AsS_2CN$-$(CH_2CH)_2$, **57**	2.702(5)	0.061	3.144(2)	0.050	2.275(2)	0.836	13.6	157.55(15)	CC	[15]
$O(CH_2CH_2S)_2AsS_2PPh_2$, **58**	2.678(5)	0.065	3.332(2)	0.027	2.286(2)	0.807	14.8	159.1(1)	CC	[44]
$O(CH_2CH_2S)_2AsS_2$-$P(OCH_2)_2CEt_2$, **59**	2.627(8)	0.077	3.537(4)	0.013	2.287(4)	0.804	11.9	162.8(3)	CC, MPC	[61]
$S(CH_2CH_2S)_2AsCl$, **60**	2.719(3)	0.198	–	–	2.356	0.547	12.2	189.5(3)	BC	[45]
$[S(CH_2CH_2S)_2As]^+[GaCl_4]^-$, **61** (molecule a and b)	2.347(10)	0.662	–	–	–	–	–	–	BB	[60]
	2.391(9)	0.574							BC	
$S(CH_2CH_2S)_2AsBr$, **62**	2.70	0.210	–	–	2.54	0.703				[46]
$S(CH_2CH_2S)_2AsI$, **63**	2.77	0.168	–	–	2.77	0.365				[46]
$S(CH_2CH_2S)_2AsS_2$-$CN(CH_2CH)_2$, **64**	3.170(2)	0.046	3.079(2)	0.061	2.306(2)	0.756	11.6	158.85(7)	BC	[15]
(molecule a and b)	3.113(2)	0.056	3.011(2)	0.076	2.307(2)	0.754	6.5	165.93(8)	BC	
$S(CH_2CH_2S)_2AsS_2CNEt_2$, **65**	3.172(2)	0.045	2.980(2)	0.085	2.305(1)	0.759	8.6	163.6(0)	BC	[43]
$S(CH_2CH_2S)_2AsS_2PPh_2$, **66**	2.881(4)	0.117	3.267(4)	0.033	2.414(3)	0.532	10.1	166.5(1)	BC	[44]
$S(CH_2CH_2S)_2AsS_2P(OMe)_2$, **67**	2.911(1)	0.106	3.326(2)	0.027	2.375(1)	0.605	9.1	168.0(1)	BC	[48]
$S(CH_2CH_2S)_2AsS_2$-$P[OCH(Me)]_2CH_2$, **68**	2.942(11)	0.096	3.486(11)	0.016	2.357(1)	0.641	10.5	168.49(4)	BC	[17]
$O(CH_2CH_2S)_2SbCl$, **69**	2.529(4)	0.191	–	–	2.448(2)	0.727	19.8	152.0(1)	CC	[52]
$O(CH_2CH_2S)_2SbPh$, **70**	2.942(4)	0.050	–	–	2.164(6)	0.895		–	CC	[51]
$O(CH_2CH_2S)_2SbS_2CN(CH_2CH)_2$, **71**	2.795(3)	0.079	3.012(1)		2.492(1)	0.742	13.0	148.52(.09)	BC	[15]
$O(CH_2CH_2S)_2SbS_2$-$CN(CH_2CH_2)_2$, **72**	2.795(3)	0.079	3.026(2)	0.073	2.492(1)	0.742	13.1	148.51(08)	BC	[17]
$O(CH_2CH_2S)_2SbS_2PPh_2$, **73**	2.555(6)	0.173	3.144(2)	0.050	2.505(3)	0.984	15.5	153.4(1)	BC	[49]
$O(CH_2CH_2S)_2SbS_2PMe2$, **74**	2.561(7)	0.173	3.332(2)	0.027	2.495(3)	0.735	13.0	154.3(2)	BC	[50]
$O(CH_2CH_2S)_2SbS_2$-$P(OCH_2)_2CEt_2$, **75**	2.608(4)	0.147	3.537(4)	0.013	2.517(2)	0.684	14.8	152.61(9)	BC	[17]
$O(CH_2CH_2S)_2SbS_2$-$P(OCH_2)_2C(Me)Pr$, **76**	2.600(2)	0.152	–	–	2.520(24)	0.677	13.2	154.16(9)	BC	[17]
$[O(CH_2CH_2S)_2Sb]_2$-$(SCH_2CH_2)_2O$, **77**	2.734(3)	0.100	–		2.452(1)	0.845	15.9	148.9(1)	CC	[59]
	2.637(4)	0.133			2.446(2)	0.861	13.6	153.3(1)	BC	
$S(CH_2CH_2S)_2SbCl$, **78**	2.832(3)	0.247	–	–	2.508(3)	0.600	11.7	162.5(2)	BC	[53]
(molecule a and b)	2.879(3)	0.210			2.521(3)	0.574	5.6	163.4(2)		
$S(CH_2CH_2S)_2SbBr$, **79**	2.86	0.022	3.079(2)	0.061	2.68	0.506		–	BC	[46]
$S(CH_2CH_2S)_2SbPh$, **80**	3.363(1)	0.044	3.011(2)	0.076	2.169(4)	0.881		–	BC	[46]
	3.308(1)	0.052	2.980(2)	0.085	2.158(4)	0.913				
$S(CH_2CH_2S)_2SbS_2$-$CN(CH_2CH)_2$, **81**	3.123(2)	0.096	3.267(4)	0.033	2.533(1)	0.649		153.12(06)	BC	[15]
$S(CH_2CH_2S)_2SbS_2$-$CN(CH_2CH_3)_2$, **82**	3.126(2)	0.097	3.326(2)	0.027	2.543(2)	0.629	7.6	156.8(1)	BC	[17]
$S(CH_2CH_2S)_2Sb(C_6H_4)NO_2$, **83**	3.189(2)	0.077	3.486(11)	0.016	2.189(5)	0.826		–	BC	[54]
$S(CH_2CH_2S)_2SbS_2PMe_2$, **84**	2.972(1)	0.157	3.147(2)	0.088	2.565(2)	0.585	8.7	159.6(1)	BC	[50]
$S(CH_2CH_2S)_2SbS_2PPh_2$, **85**	2.949(3)	0.167	3.216(3)	0.071	2.608(3)	0.509	8.5	134.9(1)	BC	[49]

[a] Bond widening, $\Delta d = (d_{exp} - \Sigma r_{Cov})$, according to standard bond distances d(As—O) 1.88, d(As—S) 2.22, d(As—Cl) 2.17, d(As—Br) 2.29, d(As—I) 2.46, d(Sb—O) 2.02, d(Sb—S) 2.40, d(Sb—Cl), d(Sb—Br) Å [9] d(Sb—C) 2.20 [62].

[b] Mode of calculation for intramolecular BO = $10^{-(1.41\Delta d)}$ [3,7].

[c] $\Delta\theta = (\theta_{eq}) - (\Sigma\theta_{ax})/2$; $\Delta\theta = 0^\circ$ for a perfect ψ-tetrahedron; $\Delta\theta = 30^\circ$ for a perfect ψ-trigonal bipyramid; cf the related $\Delta\theta$ as a parameter of the goodness of a trigonal bipyramid [1,3].

Table 3
Coordination geometry and type of molecule framework for the group 15 compounds

Compound	Type of molecule framework	Geometry[a]	References
$O(CH_2CH_2S)_2AsCl$, **53**	monomeric	Ψ-TBP (AB_4E)	[47]
$O(CH_2CH_2S)_2AsBr$, **54**	monomeric	Ψ-TBP (AB_4E)	[46]
$O(CH_2CH_2S)_2AsI$, **55**	dimeric	Ψ-octahedron (AB_4DE)	[46]
$O(CH_2CH_2S)_2AsS_2CN(CH_2CH_2)_2O$, **56**	monomeric	Ψ-monocapped SPY (AB_4E)	[43]
$O(CH_2CH_2S)_2AsS_2CN(CH_2CH)_2$, **57**	monomeric	Ψ-monocapped SPY (AB_4E)	[15]
$O(CH_2CH_2S)_2AsS_2PPh_2$, **58**	monomeric	Ψ-monocapped TBP (AB_4CE)	[44]
$O(CH_2CH_2S)_2AsS_2P(OCH_2)_2CEt_2$, **59**	monomeric	Ψ-monocapped TBP (AB_4CE)	[61]
$S(CH_2CH_2S)_2AsCl$, **60**	dimeric	Ψ-octahedron (AB_4DE)	[45]
$[S(CH_2CH_2S)_2As]^+$ $[GaCl_4]^-$, **61** molecules a and b	monomeric	Ψ-TP (AB_3)	[60]
$S(CH_2CH_2S)_2AsBr$, **62**	dimeric	Ψ-octahedron (AB_4DE)	[46]
$S(CH_2CH_2S)_2AsI$, **63**	monomeric	Ψ-TBP (AB_4E)	[46]
$S(CH_2CH_2S)_2AsS_2CN(CH_2CH)_2$, **64** molecules a and b	monomeric	Ψ-monocapped TBP (AB_4CE)	[15]
$S(CH_2CH_2S)_2AsS_2CNEt_2$, **65**	monomeric	Ψ-monocapped SPY (AB_4E)	[43]
$S(CH_2CH_2S)_2AsS_2PPh_2$, **66**	monomeric	Ψ-monocapped SPY (AB_4E)	[44]
$S(CH_2CH_2S)_2AsS_2P(OMe)_2$, **67**	monomeric	Ψ-monocapped SPY (AB_4E)	[48]
$S(CH_2CH_2S)_2AsS_2P[OCH(Me)]_2CMe_2$,**68**	monomeric	Ψ-monocapped TBP (AB_4CE)	[17]
$O(CH_2CH_2S)_2SbCl$, **69**	chain	Ψ-monocapped octahedron (AB_4D_2E)	[52]
$O(CH_2CH_2S)_2SbPh$, **70**	double chain	Ψ- monocapped octahedron (AB_4D_2E)	[51]
$O(CH_2CH_2S)_2SbS_2CN(CH_2CH)_2$,**71**	dimeric	Ψ-bicapped TBP (AB_4CDE)	[15]
$O(CH_2CH_2S)_2SbS_2CN(CH_2CH_2)_2$, **72**	dimeric	Ψ-bicapped TBP (AB_4CDE)	[17]
$O(CH_2CH_2S)_2SbS_2PPh_2$, **73**	dimeric	Ψ-bicapped TBP (AB_4CDE)	[49]
$O(CH_2CH_2S)_2SbS_2PMe_2$, **74**	dimeric	Ψ-bicapped TBP (AB_4CDE)	[50]
$O(CH_2CH_2S)_2SbS_2P(OCH_2)_2CEt_2$, **75**	dimeric	Ψ-bicapped TBP (AX_4CDE)	[17]
$O(CH_2CH_2S)_2SbS_2P(OCH_2)_2C(Me)Pr$, **76**	dimeric	Ψ-bicapped TBP (AX_4CDE)	[17]
$[O(CH_2CH_2S)_2Sb]_2(SCH_2CH_2)_2O$, **77**	dimeric	Ψ-monocapped TPB (AB_4CE)	[59]
$S(CH_2CH_2S)_2SbCl$, **78** molecules a and b	3-network	Ψ-monocapped octahedron (AB_4C_2E)	[53]
$S(CH_2CH_2S)_2SbBr$, **79**	chain	Ψ-square antiprisma (AB_4D_2E)	[46]
$S(CH_2CH_2S)_2SbPh$, **80** molecules a and b	tetrameric	Ψ-monocapped octahedron (AB_4D_2E)	[46]
$S(CH_2CH_2S)_2SbS_2CN(CH_2CH)_2$, **81**	dimeric	Ψ-bicapped TBP (AB_4CDE)	[15]
$S(CH_2CH_2S)_2SbS_2CN(CH_2CH_3)_2$, **82**	dimeric	Ψ-bicapped TBP (AB_4CDE)	[17]
$S(CH_2CH_2S)_2Sb(C_6H_4)NO_2$, **83**	dimeric	Ψ-monocapped octahedron (AB_4D_2E)	[54]
$S(CH_2CH_2S)_2SbS_2PMe_2$, **84**	dimeric	Ψ-bicapped TBP (AB_4CDE)	[50]
$S(CH_2CH_2S)_2SbS_2PPh_2$, **85**	dimeric	Ψ-bicapped TBP (AB_4CDE)	[49]
$MeN(CH_2CH_2NSiMe_3)_2BiCl$, **86**	monomer	ψ- TBP (AB_4E)	[58]
$O(CH_2CH_2S)_2BiPh$, **87**	2^d-polymeric chain	ψ-monocapped octahedron (AX_4D_2E)	[55]
$S(CH_2CH_2S)_2BiCl$, **88**	dimeric	ψ-monocapped octahedron (AX_4D_2E)	[56]
$S(CH_2CH_2S)_2BiS(CH_2CH_2)NH_2$, **89**	monomeric, polymeric	ψ-monocapped TBP (AD_4CE)	[57]
$S(CH_2CH_2S)_2BiS(C_6H_5)CO_2Me$, **90**	monomeric	ψ-monocapped TBP (AD_4CE)	[57]
$[S(CH_2CH_2S)_2BiSCH_2CH_2]_2S$, **91**	polymeric	ψ-monocapped octahedron (AB_3D_3E)ψ-monocapped TBP (AB_4D_2E)	[56]

[a] A = Sb or As, B = normal bond and transannular atoms, C = additional intramolecular secondary bonding to Sb or As, D = intermolecular contacts and E = lone pair.

388°; thus these compounds do not obey the Berry coordinate.

On the other hand, taking into account the stereochemically-active lone pair (which commonly occupies an equatorial position), the metal center in these compounds can be described as a ψ-TBP. If the exocyclic secondary bonding is also taken into account, the arsocanes become pentacoordinate exhibiting a continuous series of distorted geometries extending from ψ-monocapped TBP to ψ-monocapped SPY or rectangular pyramids. In this regard, the metal center in compounds $O(CH_2CH_2S)_2AsS_2PPh_2$ (**58**) and $O(CH_2CH_2S)_2AsS_2P(OCH_2)_2CEt_2$ (**59**) is best described as a ψ-monocapped TBP, while $O(CH_2CH_2S)_2AsS_2CN(CH_2CH_2)_2O$ (**56**), $O(CH_2CH_2S)_2AsS_2CN(CH_2CH)_2$ (**57**), $S(CH_2CH_2S)_2AsS_2CNEt_2$ (**65**), $S(CH_2CH_2S)_2AsS_2PPh_2$ (**66**) and $S(CH_2CH_2S)_2AsS_2P(OMe)_2$ (**67**) display geometries that are closer to a ψ-monocapped SPY (Table 3).

The arsocanes **55**, **60** and **62** exist as interesting dimers in solid state and exhibit a ψ-octahedral geometry [AB_4DE, A = As, B = transannular atom and normal bonds, D = intermolecular contacts, E = lone pair]. Other arsocanes exist as discrete molecular units separated by normal van der Waals distances in their solid-state framework. This behavior contrasts the higher associated frameworks encountered for the heavier metallocanes of the same family.

Arsocanes offer examples of the three extreme boat–boat, boat–chair and chair–chair conformations. Compound $[S(CH_2CH_2S)_2As]^+[GaCl_4]^-$ (**61**) is the only known example of a discrete arsenium cation, where **61a** and **61b** cor-

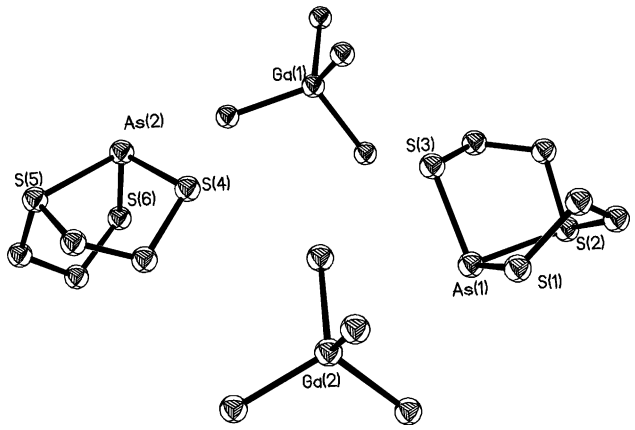

Fig. 3. Molecular structures of $[S(CH_2CH_2S)_2As]^+[GaCl_4]^-$ (**61**, molecules a and b).

respond to two crystallographically independent molecules that differ in the conformation of their eight-membered ring (Fig. 3). Molecule **61a** possesses a boat–boat conformation with a BO of 0.662 for the S···As interaction, whilst, molecule **61b** exhibits a boat–chair conformation with a BO of 0.574. The bond orders for these As···S transannular interactions represent the highest known values for any reported arsocane. This behavior can be attributed to the heterolytic As–Cl cleavage that promotes the formation of the transannular As···S bond, and clearly demonstrates that the magnitude of the BO in the transannular (M···X) interaction is not the sole factor governing the conformation of the eight-membered ring, other factors such as crystalline packing should considered.

3.2. Antimony(III) metallocanes

Stibocanes represent a well-studied group, where the general tendency in the strength of the M···X interaction can be regarded as similar to that observed in arsocanes. The halogen-containing stibocanes $[O(CH_2CH_2S)_2]SbCl$ (**69**), $[S(CH_2CH_2S)_2]SbR$ (R = Cl) (**78**) and (R = Br) (**79**) exhibit stronger transannular interactions than those found in their dithiolate and organometallic derivatives (Table 2). Though not in the scope of this review, eight-membered organometallic stibocanes, $X(CH_2CH_2CH_2)_2SbR$ (X = NMe, NBz; R = Cl, I, NCS) [6] exhibit stronger 1,5-transannular interactions (BO 0.39–0.53) when compared to 1-oxa-4,6-dithia- and 1,3,6-trithia- stibocanes (X = O, S; R = Cl, Br, with BOs ranging from 0.19 to 0.25). This tendency is in agreement with that observed in Sn(IV) homologues (Section 2.1).

The molecular structures of stibocanes are known to exhibit three general types of secondary bonding; 1,5-transannular bonding, stretched exocyclic chelation (namely with dithiolate type ligands) and short intermolecular interactions that lead to higher association frameworks (Table 3). When transannular bonding is taken into account, the antimony atom becomes tetracoordinate, exhibiting a distorted trigonal bipyramidal (TBP) VSEPR geometry,

Table 4
Structural features of the three center interaction X···Bi–R_{ax} for the bismocanes, $X(CH_2CH_2Y)_2BiR$

Compound	d(Bi···X)[a] Å	BO[b] Bi···X	d(Bi–R_{ax})[a] Å	BO[b] Bi–R_{ax}	d(Bi···[Z])[a]	BO[c] Bi···[Z]	$\Delta\theta$[d] (deg.)	X···i–R_{ax} (deg.)	Conformation	References
$MeN(CH_2CH_2NSiMe_3)_2BiCl$, **86**	2.496(6)	0.450	2.6727(17)	0.650	3.725(1) *[Cl]*, 3.732 (1) *[Bi]*	0.090, 0.282	9.6	159.60(14)	BC	[58]
$O(CH_2CH_2S)_2BiPh$, **87**	2.971(1)	0.084	2.250(2)	1.255	3.440(3) *[S]*, 3.509(3) *[S]*	0.178, 0.154	15.5	141.2(4)	CC	[55]
$S(CH_2CH_2S)_2BiCl$, **88**	2.848(5)	0.433	3.012(1)	0.216	3.524(6) *[S]*, 4.220(5) *[Bi]*	0.150, 0.103	14.2	155.35(14)	BB	[56]
$S(CH_2CH_2S)_2$-$BiSCH_2CH_2NH_2$, **89**	3.247(2)	0.118	2.596(6)	0.981	–	–	3.4	155.5	BC	[57]
$S(CH_2CH_2S)_2$-$BiS(C_6H_5)CO_2Me$, **90**	3.067(4)	0.212	2.602(9)	0.962	3.445(8) *[S]*	0.176	12.8	154.95(14)	BC	[57]
$[S(CH_2CH_2S)_2$-$BiSCH_2CH_2]_2S$, **91**	3.071(5)	0.210	2.615(21)	0.922	4.239(6) *[Bi]*, 3.261(3) *[S]*	0.099, 0.256	0.2	162.07(14)	BC	[56]
					3.933(3) *[S]*	0.065				
	3.197(3)	0.139	2.566(30)	0.925	3.191(2) *[S]*, 3.806(4) *[S]*	0.295, 0.085	6.3	152.29(15)	BC	

[a] Bond widening, $\Delta d = (d_{exp} - \Sigma r_{Cov})$, according to standard bond distances d(Bi—C), d(Bi—N) 2.25, d(Bi—O) 2.21, d(Bi—S) 2.59, d(Bi—Cl) 2.54, d(Bi—Br) 3.10 [6], d(Bi—C) [9,58].
[b] Mode of calculation for intramolecular $BO = 10^{-(1.41\Delta d)}$ [3,7].
[c] Mode of calculation for intermolecular $BO = 10^{-(1.4\Delta d/1.6)}$ [3,7].
[d] $\Delta\theta = (\theta_{eq}) - (\Sigma\theta_{ax})/2$; $\Delta\theta = 0°$ for a perfect ψ-tetrahedron; $\Delta\theta = 30°$ for a perfect ψ-trigonal bipyramid; cf the related $\Delta\theta$ as a parameter of the goodness of a trigonal bipyramid [1,3].

with the lone pair and two heteroatoms attached to the metal center (within the eight-membered ring) occupying the equatorial positions and the transannular atom, and the exocyclic ligand (halogen or organic group) occupying the axial positions. If intermolecular contacts are present, the antimony atom can acquire higher coordination numbers with geometrical arrangements such as Ψ-bicapped TPB and Ψ-monocapped octahedra. In the later case, the exocyclic R ligand and the X donor occupy the axial positions. While, two sulfur atoms from the eight-membered ring and one or two intermolecular contacts occupy the equatorial positions, with the lone pair capping one of the edges.

On the other hand, the geometry around the metal center in monomeric dithiolate-containing stibocanes can be described as a Ψ-monocapped TBP [AB_4CE, A = Sb, B = normal covalent bonds or transannular atoms, C = intramolecular exocyclic bonding and E = lone pair]. In contrast, when intermolecular interactions are present, the antimony atom commonly displays Ψ-bicapped TBP geometries (AB_4CDE, A = Sb, B = normal covalent bonds or transannular atoms, C = intramolecular exocyclic bonding, D = intermolecular contact and E = lone pair).

Finally, 1-oxa-4,6-dithia-stibocanes exist exclusively as boat–chair conformers, with the exception of $O(CH_2CH_2S)_2SbCl$ (**69**) and $O(CH_2CH_2S)_2SbPh$ (**70**), which exhibit chair–chair conformations. On the other hand, 1,3,6-trithia-stibocanes exhibit solely boat–chair conformations with the exception of $[O(CH_2CH_2S)_2Sb]_2$-$(SCH_2CH_2)_2O$ (**77**), which contains two metallocane moieties, exhibiting a boat–chair and a chair–chair conformation in the same molecule.

3.3. Bismuth(III) metallocanes

The structural features of bismocanes represent a developing database, with few bismocane structures known to date. Nonetheless, these exhibit a much broader structural diversity than the lighter members of the same family. The most important structural features of the complexes are summarized in Tables 3 and 4. Geometry, coordination number, solid-state framework and the conformation of the eight-membered ring vary considerably through the series of bismocanes.

Compound $MeN(CH_2CH_2NSiMe_3)_2BiCl$ (**86**) exhibits a strong Bi···N transannular interaction [2.496(6) Å, BO 0.450] with a boat–chair conformation in the eight-membered ring (Fig. 4). This behavior, as well as the existence of low aggregation forms for **86** can be regarded as a direct consequence of the steric bulkiness of the trimethylsilyl groups present in the molecule. In this regard, the short intermolecular Bi···Bi contact (3.731 Å, BO 0.282) in its solid-state framework may indicate a dimeric arrangement. Nonetheless, the small value for the N(1)–Bi–N(3) angle (69.13°) suggests that this compound is best regarded as a discrete monomer. The coordination geometry around bismuth corresponds to a TBP, where the small equatorial N(1)–Bi–N(3) angle (101.8°) indicates the strong *s*-character of the lone pair.

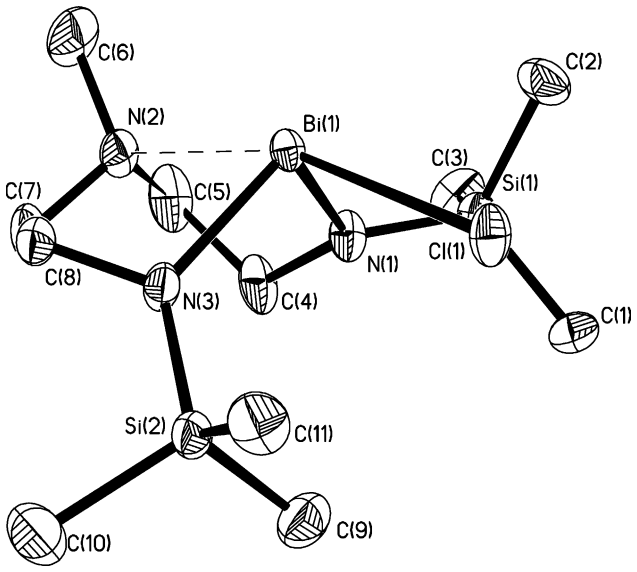

Fig. 4. Molecular structure of $MeN(CH_2CH_2NSiMe_3)_2BiCl$ (**86**).

On the other hand, $O(CH_2CH_2S)_2BiPh$ (87) represents the only known example of an organometallic bismocane. This 1-oxa-4,6-dithia-bismocane exhibits a very weak Bi···O transannular interaction (BO 0.084), slightly stronger than its stibocane homologue **70** (BO 0.050), yet both compounds adopt a chair–chair conformation. Taking into account the transannular bonding and the two intermolecular contacts [Bi···S 3.440(3) and 3.509(3) Å], the metal center exhibits a ψ-monocapped octahedral geometry. The polyhedra are connected through two edges and the crystal structure exhibits a two-dimension chain framework.

$S(CH_2CH_2S)_2BiCl$ (**88**) is the only bismocane that exhibits a boat–boat conformation. In this compound, the Bi···S transannular BO is similar to the transanular Bi···N bonding for **86** (0.433 and 0.450, respectively).

An unusual and interesting crystal structure was observed for $S(CH_2CH_2S)_2BiS(CH_2CH_2)NH_2$ (**89**), which exhibits both a monomeric species (**89a**; Fig. 5) as well as polymeric chains through association by one of the S atoms that would be expected to form an eight-membered ring (**89b**, Fig. 5). The monomeric structure exhibits a boat–chair conformation and the BO value for the transannular Bi···S interaction is 0.118.

Other examples of bismocane structures include $S(CH_2CH_2S)_2BiS(C_6H_5)CO_2Me$ (**90**) and $S(CH_2CH_2S)_2$-$BiSCH_2CH_2]_2S$ (**91**), which exhibit almost identical BO values for the transannular Bi···S contact (0.212 and 0.210, respectively), and the same boat–chair conformation. Additionally, **91** exhibits two metallocane moieties in the same molecule, each with a boat–chair conformation. The intramolecular and intermolecular contacts provide for six- and seven-coordinate bismuth environments in the same molecule.

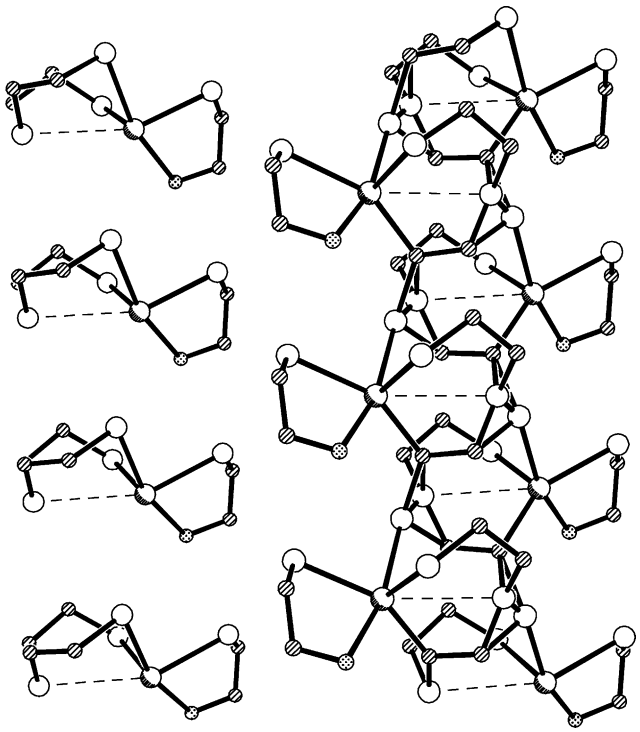

Fig. 5. Solid-state framework of $S(CH_2CH_2S)_2BiS(CH_2CH_2)NH_2$ (**89**).

4. Conclusions

Regardless of the nature of the L ligands and the nature of the X element, the group 14 and 15 metallocanes investigated by X-ray diffraction exhibit some common structural features: a) the 1,3,6-trithia-metallocanes possess stronger transannular secondary bonding in comparison with the 1-oxa-4,6-dithia-metallocanes; b) complexes containing bidentate ligands coordinate in a monometallic anisobidentate mode with one primary M–S1(L) bond and a secondary M···S2(L) interaction. As a consequence of the additional exocyclic bonding, a weakening in the transannular bonding is observed and the coordination around the metal atom becomes highly distorted.

The M···X interaction determining the position of the metal along the pathway trigonal-bipyramid ↔ tetrahedron depends strongly on the electronegativity of Y and R groups and on the nature of the of the X atom. In general, the solid-state date indicate a sequence of the donor strength of the X donor atom in the order $MeN > S \geq O$. The comparison between the BO (M···X) and BO ($M\cdots R_{ax}$) provides further evidence for the factors that affect the nucleophilic attack at the σ-Lewis acidic M. The irregular trends observed in these groups bring to light the importance of the two different types of metal acidity: σ-acidity with regard to the intermolecular donor atom and π-acidity with regard to the ligands. The sequences in both types of acidities might not change to the same degree, thus giving rise to some of these irregular trends.

Further research can be anticipated regarding variations in the nature of the exocyclic ligands and in the atoms attached to the metal center within the eight-membered ring. The heavier members of both families are expected to exhibit unusual supramolecular associations.

References

[1] U. Kolb, M. Beuter, M. Dräger, Inorg. Chem. 33 (1994) 4522.
[2] M. Dräger, Z. Anorg. Allg. Chem. 411 (1975) 79.
[3] U. Kolb, M. Beuter, M. Gerner, M. Dräger, Organometallics 13 (1994) 4413.
[4] K. Jurkschat, J. Schilling, C. Mügge, A. Tzshach, J. Meunier-Piret, M. van Meerssche, M. Gielen, R. Willen, Organometallics 7 (1988) 38.
[5] M. Beuter, U. Kolb, A. Zickgraf, E. Bräu, M. Bletz, M. Dräger, Polyhedron 16 (1997) 4005.
[6] E. Bräu, A. Zickgraf, M. Dräger, E. Mocellin, M. Maeda, M. Takahashi, M. Takeda, C. Mealli, Polyhedron 17 (1998) 2655.
[7] L. Pauling, The Nature of the Chemical Bond, third ed., Cornell University Press, Ithaca, NY, 1960, p. 239.
[8] M. Dräger, J. Organomet. Chem. 251 (1983) 209.
[9] N.W. Alcock, Adv. Inorg. Chem. Radiochem. 15 (1972) 1.
[10] M. Dräger, Z. Naturforsch. 40B (1985) 1511.
[11] M. Dräger, H.J. Guttmann, J. Organomet. Chem. 212 (1981) 171.
[12] M. Dräger, Chem. Ber. 114 (1981) 2055.
[13] M. Dräger, Z. Naturforsch. 36b (1981) 437.
[14] M. Dräger, Z. Anorg. Allg. Chem. 527 (1985) 169.
[15] R. Cea-Olivares, et al, unpublished work.
[16] R. Cea-Olivares, V. García-Montalvo, R.A. Toscano, A. Gómez-Ortíz, R. Ferrari-Zijlstra, P. García y García, A.M. Cotero-Villegas, M. López-Cardoso, Rev. Soc. Quim. Mex. 44 (2000) 176.
[17] P. García y García, et al, unpublished work.
[18] P. García y García, R. Cruz-Almanza, R.A. Toscano, R. Cea-Olivares, J. Organomet. Chem. 598 (2000) 160.
[19] O. Jung, J.H. Jeong, Y.S. Sohn, Organometallics 10 (1991) 761.
[20] R. Cea-Olivares, V. Lomelí, S. Hernández-Ortega, I. Haiduc, Polyhedron 14 (1995) 747.
[21] V. García-Montalvo, et al, unpublished work.
[22] Z. Jian-Jun, D. Wen-Xin, H. Sheng-Min, X. Sheng-Qing, W. Long-Sheng, W. Xin-Tao, Inorg. Chem. Commun. 6 (2003) 387.
[23] R.G. Swisher, R.R. Holmes, Organometallics 3 (1984) 365.
[24] C. Mügge, K. Jurkschat, A. Tzschach, A. Zschunke, J. Organomet. Chem. 164 (1979) 135.
[25] M. Dräger, Z Anorg. Allg. Chem. 423 (1976) 53.
[26] M. Dräger, L. Ross, Chem. Ber. 108 (1975) 1712.
[27] C. Deng-Hai, C. Hung-Cheh, U. Chuen-Her, Inorg. Chim. Acta 208 (1993) 99.
[28] S. Gurkova, A.I. Gusev, N.V. Alekseev, T.K. Gar, N.A. Viktorov, Zh. Struk. Khim. 31 (1990) 158.
[29] C. Deng-Hai, C. Hung-Cheh, J. Chin. Chem. Soc. 40 (1993) 373.
[30] C. Hung-Cheh, L. Su-Mi, U. Chuen-Her, Acta Cryst. C48 (1992) 993.
[31] M. Dräger, N. Kleiner, Z. Anorg. Allg. Chem. 522 (1985) 48.
[32] P. García y García, A.M. Cotero-Villegas, M. López-Cardoso, V. García-Montalvo, R.A. Toscano, A. Gómez-Ortíz, R. Ferrari-Zijlstra, R. Cea-Olivares, J. Organomet. Chem. 587 (1999) 215.
[33] R. Fiedler, H. Follner, Monatsch. Chem. 108 (1977) 319.
[34] H. Follner, Monatsch. Chem. 103 (1972) 1438.
[35] J.W. Turley, F.P. Boer, J. Am. Chem. Soc. 90 (1968) 4026.
[36] H. Follner, Monatsch. Chem. 102 (1971) 245.
[37] H. Follner, Z. Anorg. Allg. Chem. 387 (1972) 43.
[38] R. Willem, M. Gielen, J. Meunier-Piret, M. van Meerssche, K. Jurkschat, A. Tzshach, J. Organomet. Chem. 277 (1984) 335.
[39] A. Zickgraf, M. Beuter, U. Kolb, M. Dräger, R. Tozer, D. Dakternieks, K. Jurkschat, Inorg. Chim. Acta 275–276 (1998) 203.

[40] A. Tzshach, K. Jurkschat, M. Scheer, J. Meunier-Piret, M. van Meerssche, J. Organomet. Chem. 259 (1983) 165.
[41] K. Jurkschat, A.M. Scheer, J. Tzshach, M. Meunier-Piret, van Meerssche, J. Organomet. Chem. 281 (1985) 173.
[42] L.J. Muetterties, L.J. Guggenberger, J. Am. Chem. Soc. 99 (1985) 3318.
[43] R. Cea-Olivares, M.R. Estrada, G. Espinosa-Pérez, I. Haiduc, P. García y García, M. López-Cardoso, M. López-Vaca, Main Group Chem. 1 (1995) 159.
[44] M.A. Muñoz-Hernández, R. Cea-Olivares, G. Espinosa-Pérez, S. Hernández-Ortega, Dalton Trans. (1996) 4135.
[45] M. Dräger, Chem. Ber. 107 (1974) 2601.
[46] M. Dräger, W. Hafner, H.M. Hoffmann, Z. Kristallogr. 152 (1982) 33.
[47] M. Dräger, Z. Anorg. Allg. Chem. 411 (1975) 79.
[48] M.A. Muñoz-Hernández, R. Cea-Olivares, S. Hernández-Ortega, Inorg. Chim. Acta 253 (1996) 31.
[49] M.A. Muñoz-Hernández, R. Cea-Olivares, S. Hernández-Ortega, Z. Anorg. Allg. Chem. 622 (1996) 1392.
[50] M.A. Muñoz-Hernández, R. Cea-Olivares, S. Hernández-Ortega, Z. Anorg. Allg. Chem. 623 (1997) 642.
[51] M. Dräger, H.M. Hoffmann, J. Organomet. Chem. 295 (1985) 33.
[52] M. Dräger, Z. Anorg. Allg. Chem. 424 (1976) 183.
[53] M. Dräger, Z. Anorg. Allg. Chem. 405 (1974) 183.
[54] M. Dräger, H.M. Hoffmann, J. Organomet. Chem. 320 (1987) 273.
[55] M. Dräger, B.M. Schmidt, J. Organomet. Chem. 290 (1985) 133.
[56] L. Agocs, N. Burford, T.S. Cameron, J.M. Curtis, J.F. Richardson, K.N. Robertson, Y. Yhard, J. Am. Chem. Soc. 126 (1996) 895.
[57] L. Agocs, G.G. Briand, N. Burford, M.D. Eelman, N. Aumeerally, D. MacKay, K.N. Robertson, T.S. Cameron, Can. J. Chem. 81 (2003) 632.
[58] J.L. Fauré, H. Gornitzka, R. Réau, D. Stalke, G. Bertrand, Eur. J. Inorg. Chem. (1999) 2295.
[59] R. Cea-Olivares, M.A. Muñoz-Hernández, S. Hernández-Ortega, C. Silvestru, Inorg. Chim. Acta 236 (1995) 31.
[60] N. Burford, T.M. Parks, P.K. Bakashi, T.S. Cameron, Angew. Chem. Int. Ed. 33 (1994) 1267.
[61] P. García y García, R. Cruz-Almanza, S. Hernández-Ortega, R. Cea-Olivares, Rev. Roum. Chim. 47 (2002) 1047.
[62] J.E. Huheey, E.A. Keiter, R.L. Keiter, Inorganic Chemistry. Principles of Structure and Reactivity, fourth ed., Harper & Collin, New York, 1993, p. 291.